TIJMET 002 (2019) 01-07
The International Journal of
Materials and Engineering Technology

ISSN: 2667-4033
TIJMET ID: 190201001 (7 pages)
Type of the Paper: Article
Received 07.01.2019 Revised: 06.02.2019 Accepted: 06.02.2019 Published (Online): 08.02.2019
Journal homepage: http://dergipark.gov.tr/tijmet

PRODUCTION OF FERRIC COMPLEX COMPOUNDS FOR WASTEWATER TREATMENT FROM HOT ROLLED IRON-STEEL SOLID WASTE

ELİF UZUN[*1]

[1]Department of Metallurgy and Materials Engineering, Marmara University, 34722, Istanbul, Turkey
E-mail: elif.uzun@marmara.edu.tr

Abstract

Study on oxide scales of products is of greater importance to manufacturers and consumers. These secondary and tertiary scales must be recycled because of high iron content. If these residues are not effectively treated, not only the environment will be seriously polluted, but also the resources will be wasted. In this study, the extraction of iron from Turkish hot rolled iron-steel oxide scale was attempted using atmospheric acid leaching. The effects of the several parameters which included solid/liquid ratio, leaching time, leaching temperature and acid concentration upon leaching efficiency of iron were investigated. The volumetric titration results showed that the amount of Fe^{+2} and Fe^{+3} could reach respectively 47% and %38 at 60°C temperature in 6N HCl acid concentration during 60 minutes leaching time. Two alternative methods which were atmospheric evaporation and alkaline precipitation have been successfully applied by using leaching solution as iron chloride source. The experimental results show that $FeCl_3$ was obtained by atmospheric evaporation method with a small amount of $FeCl_2$. Alkaline precipitation method's results show that the iron was existed in ferric hydroxide formation. Both precipitate and crystalized products have been iron products which are frequently used as an adsorbent to remove various heavy metals (i.e., arsenic and chromium) from contaminated soil and water and also flocculation agent.

Keyword: ferric hydroxide, Iron (III) chloride, oxide scale, hydrometallurgy.

1. Introduction

Industrial wastes are usually in solid and liquid phases. Nowadays waste treatment has gained an important dimension because of global warming, sea pollution, air pollution etc. are adversely affects life quality. On the one hand when solid wastes are recycled to a new product, on the other hand wastewater treatment facilities have been built to remove biological and chemical waste from water as it is used. Adsorption and coagulation are the most important steps in water treatment Coagulation purpose is to destabilize the dissolved contaminants or to adsorb the metal ions its solid body in water, so they may be removed by subsequent processes [1].

Classical coagulation is usually done by the addition of metallic salts especially iron salts to the water [2]. The mechanisms of coagulation for metal salts (Fe (III) salts) are a function of the hydrolysis speciation of Fe (III) ions in water [3, 4, 5, 6, 7]. In hydrolysis metal ions cause to produce unstable contaminations in the solution. The unstable contaminants are then grow together into contact with one another so that aggregation occurs. Ferric chloride and ferric hydroxide becomes more acceptable on water treatment because it shows an effective solution for destabilization of particles, removal of dissolved organic matter, and induction of flocculation and also improvement of filtration [8].

The following possible hydrolysis reactions of Fe (III) in aqueous solution were reported by Stumm and coworkers [3, 4, 9]:

$Fe^{3+} + H_2O <=> Fe(OH)^{2+} + H^+$
$Fe^{3+} + 2H_2O <=> Fe(OH)_2{}^{+} + 2H^+$
$2Fe^{3+} + 2H_2O <=> Fe2(OH)_2{}^{4+} + 2H^+$
$3Fe^{3+} + 4H_2O <=> Fe3(OH)_4{}^{5+} + 4H^+$
$Fe^{3+} + 3H_2O <=> Fe(OH)_3 + 3H^+$

Similar reactions were reported by California Water Technologies 2004 [10]. All of these reactions follow the general expression

$$xFe^{3+} + yH2O <=> Fe_x(OH)_y\ (3x-y)^+ + yH^+$$

Fe^{3+} does not exist in natural waters as a simple ion but exists as an aqua-complex species, such as $Fe(H_2O)_6{}^{3+}$.

Many inactive materials such as oxide scales occur while the production process in iron and steel hot rolled industry. The formation of oxide scales on steel at high temperatures usually consists of hematite (Fe_2O_3), magnetite (Fe_3O_4) and wustite (FeO), with the ratio of 1:4:95 [11]. The thickness of these three phases will be different with the changes of oxidation conditions, steel compositions [12, 13] and surface finish [14, 15]. Oxide scales are recycled by sinter furnaces as an iron source in integrated plants, while there is no recovery in hot rolling plants because of machinery constraints.

In this study, it has been studied on the production of $FeCl_3$ and ferric hydroxide from iron-steel hot rolled scales which cannot be considered as a source with a small scale and economic process. Atmospheric acid leaching experiments were done at different temperatures, acid concentrations and leaching time for the optimization of iron extraction. After leaching optimization experiments, evaporation and chemical precipitation methods were applied to produce $FeCl_3$ and ferric hydroxide that are waste water treatment chemicals in the industrial scale.

2. Materials and Methods

The primary objective of the present studies was to determine the dissolution behavior of oxide scales by hydrochloric acid leach under atmospheric conditions. In these experimental studies, hydrochloric acid (37%, d:1.19 g/cm^3) and de-ionized water were used. Chemical analysis of Fe was carried out with a x-ray fluorescence machine. Solid samples were also analyzed by x-ray diffractometer (XRD) (brand name: Shimadzu XRD-6100) and scanning electron microscope (SEM) with EDX (brand name: FEI Sirion XL-30 (FEG)) analyzer. Leaching experiments were performed in an 800 mL Pyrex reactor, using the batch method. The reactor was placed in a bath, whose temperature was controlled by a temperature controller via a thermocouple within an error of ± 1 °C. The agitation of the leach pulp was continuously maintained by an external propeller, rotated at a constant speed of 350 rpm throughout the processes. The complete system is shown in Figure 1.

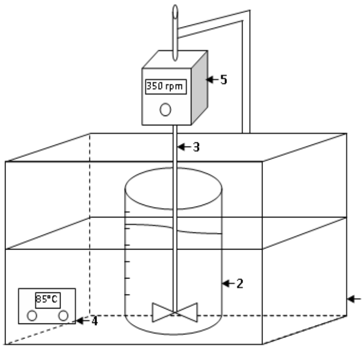

Figure 1. Experimental procedure (1: Leach Bath, 2: Pyrex Reactor, 3: Mixer, 4: Thermocouple, 5: Mixer Control).

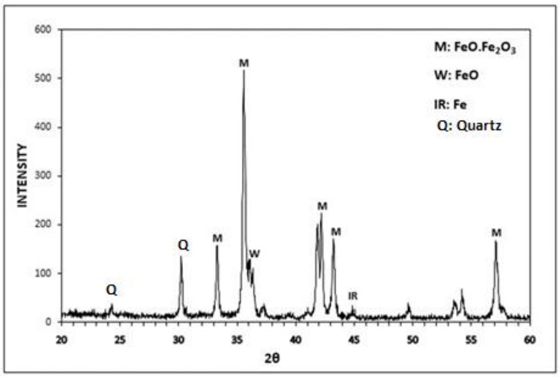

Figure 2. XRD pattern of oxide scale sample.

The optimization of leaching experiments were done different acid concentrations (1N, 3N, 6N), temperatures (room, 45°C, 60°C), leaching time (30', 60', 90') with a constant stirring velocity (350 rpm) and solid liquid ratio (1:6 w/v). Two alternative methods which were atmospheric evaporation and alkaline precipitation have been successfully applied by using pregnant leach solution as iron(III) ion source. Production of iron(III) chloride was done by atmospheric evaporation method with in a 300ml Pyrex reactor that was continuously heated until the yellow-brownish crystal phase appears. After the evaporation process, crystalline solid phase was washed with absolute ethanol and dried in a furnace at 60°C for 8 hours. Hydroxide precipitation is performed by adding reagents such as lime suspension to pregnant solution to precipitate the iron ions as iron hydroxide but a higher pH is required if the iron is in the ferrous state. A pH of 3.5 is sufficient to precipitate iron in the ferric state [16]. Parameters such as temperature and pH influence precipitate properties like filtration efficiency and particle morphology. In general, this method yields fine and gelatinous precipitate, which filters slowly and can cause valuable ions losses through co-precipitation with the iron [17]. In hydroxide precipitation, ferric hydroxide is formed at pH of around 3. The results demonstrate that precipitating agents (calcium carbonate) could be used for increasing the pH and the iron removal efficiency by using either would be the same; however, the properties of precipitates were somewhat different but the main effect of the agents are to adjust the pH in solution. In this study precipitation was done by calcium carbonate suspension (lime pulp) addition to the pregnant leach solution to increase the pH value range to 3,0 -12,00 from 0,30 because of due to the existence of both ferric and ferrous ions. Solid liquid separation was done by a vacuum pump with white band filtration paper for both methods.

2.1. Characterization of Sample

Approximately 20 kg of sample was taken from the Karabük/Turkey iron and steel hot rolling plant waste well. The chemical composition of the sample, as analyzed by EDX is shown in Table 1. The XRD pattern of the oxide scale sample, given in Figure 2, shows that magnetite metallic iron, quartz and wustite are the main phases in the sample. As can be seen in Figure 2, no hematite or other metal peaks are seen in the XRD pattern was found [18].

The morphologies and sizes of the samples were investigated by scanning electron microscope (SEM). Among them, Figure 3a, 3b, 3c are the images of the iron oxide scale. In Figure 3a oxide scales are formed in lamellar shapes because of the stripping process. As it can be seen in the same figure scales are very brittle and thin lamellar and plate form. It can be seen that the melted iron is irregularly shapes, which may result from hot rolling process [19, 20], and a little residual island oxide still exists inside oxide scale. The iron oxide scale displayed the irregular shapes and some nanoparticles adhered on the plates aggregated by other sized particles. It can be seen from the Figure 3b and 3c that the reduced iron is porous irregularly [11]. One can see that the metallic iron was greatly different form that is presented in melted form in Figure 3c shows a considerable portion of particles grown as orthogonal or cornered (angular shaped).

From the EDX analysis of iron, oxide and silicon were found in the sample (Fig 3d). In mapping figure iron ratio was the highest from the oxygen and silicon because of the metallic iron existence in the sample (Fig 3e) [21-23].

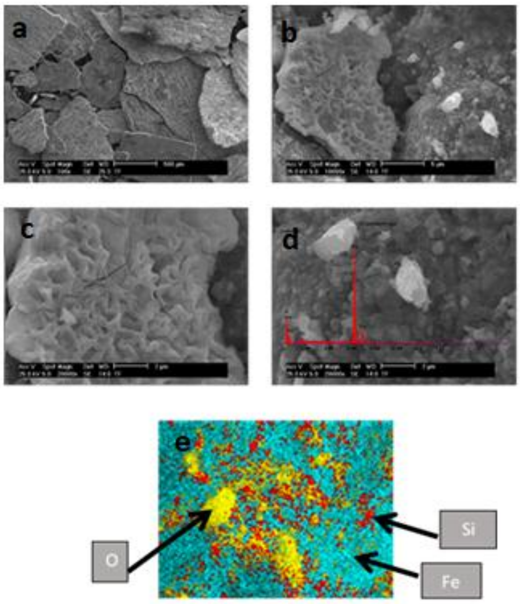

Figure 3. SEM images of oxide scale (sample) a. 100X SEM image, b.10000X SEM image, c.20000X SEM image, d. EDX of sample e. Elemental mapping of sample

Table 1. Chemical composition of oxide scale sample.

Material	**Chemical Composition, %**		
	Fe	**Si**	**O**
Oxide Scale	70,88	3,27	25,85

3. Results and Discussion

Atmospheric acid leaching experiments and results

The optimization of leaching experiments were done different acid concentrations (1N, 3N, 6N), temperatures (room, 45°C, 60°C), leaching time (30', 60', 90') with a constant stirring value (350 rpm) and solid liquid ratio (1:6 w/v). Leaching experiments were carried out 6N hydrochloric acid concentration at a leaching time of 60 minutes, at the 45°C temperature conditions. In leaching experiments solid liquid ratio was set at 1:6 weight per volume. Oxide scale and the leach residue XRD patterns were compared each other in Figure 4. As we can see from the patterns in which the raw oxide scale and leach residue were compared, the vustite contained in the sample was completely dissolved. The magnetite peak's intensity of leach residue was lower than before leaching of sample that is because magnetite is also dissolved. The fact that the intensity of metallic iron in the leach residue is higher than all other peaks is an indication that leaching conditions cannot dissolve metallic iron. The fact that existence of silicon in the leach residue that is confirm the selective beneficiation is achieved of the raw oxide scale sample. It has been found that the source of the iron ions in the pregnant leach solution comes from magnetite and wustite phases.

The volumetric titration with NaOH results showed that the amount of Fe^{+2} and Fe^{+3} could reach respectively %47 and %38 at 60°C temperature in 6N HCl acid concentration during 60 minutes leaching time.

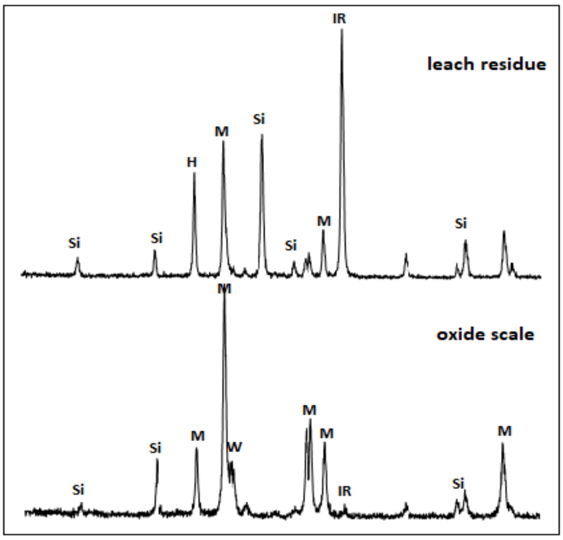

Figure 4. XRD patterns of raw oxide scale sample and leach residue of oxide scale.

3.1. Iron(III) chloride production experiments and results

Production of iron(III) chloride was done by atmospheric evaporation method with in a 300ml Pyrex reactor that was continuously heated until the yellow-brownish crystal phase appears. After the evaporation process, crystalline solid phase was washed with absolute ethanol and dried in a furnace at 60°C for 8 hours. XRD, SEM and EDX analyzes were performed for the obtained solid phase (Figure 5, Figure 6).

$FeCl_3$ peaks were observed at 21ϴ, 33ϴ and 34ϴ as shown in Figure 5. As can be seen from the XRD pattern, production of iron(III) chloride was achieved [24]. Energy dispersive X-ray spectroscopy (EDX) revealed the product of evaporated pregnant solution contained only Fe and Cl and a little oxygen elements. SEM images of the solid phase $FeCl_3$ that was obtained by evaporation process were taken. As it can be understood from the images, the lamellar structure which is in the oxide scale sample has been disappeared [25]. In the process of evaporation of the optimum pregnant solution, it was also supported by the EDX analysis where the large amount of solution transforming to the gas phase (H_2, H_2O, Cl_2) was removed and the remaining chlorine formed by Fe^{+3} ion and $FeCl_3$. The formation of $FeCl_3$ by evaporation method is clearly seen in Figure 6 where it is formed by re-crystallization formation because of the high temperature conditions. In addition, it was observed that the grain structure was not granular but needles, nodular and integrated in Figure 6c and Figure 6d.

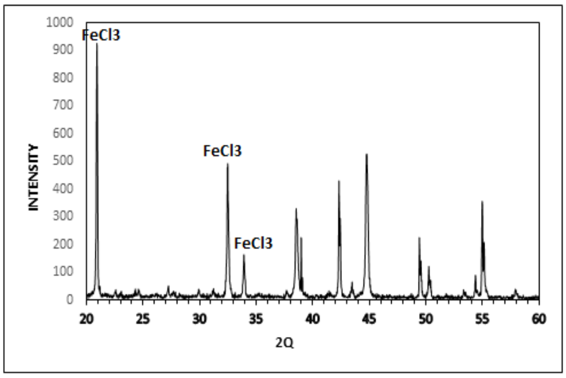

Figure 5. XRD pattern of evaporated pregnant solution.

3.2. Ferric hydroxide production experiments and results

In this experimental series, alkaline precipitation method is used to product of ferric hydroxide from the acidic iron pregnant solution. Addition of industrial lime ($CaCO_3$) to acidic iron pregnant solution will raise its pH, accelerate the rate of chemical oxidation of ferrous iron (for which active aeration, or addition of a chemical oxidising agent such as hydrogen peroxide, is also necessary), and cause many of the metals present in solution to precipitate as hydroxides and carbonates. Ferric iron can also be present in flows with pH values less than 3,5. However there is not only Fe^{+3} ions but also Fe^{+2} ions in the pregnant solution intended for precipitation. Therefore lime pulp was added until the pH value was 11.5. The XRD pattern of the precipitate is shown in the Figure 7. The analysis reveals that ferric hydroxide was obtained at 29θ, 43θ, 45θ, 48θ and 57θ peaks by alkaline precipitation method [26]. As seen in the SEM images the particles have a quasi-spherical shape and occur in the form of clusters (Figure 8). Agglomeration was seen because of precipitation process. The particles appeared more granular than $FeCl_3$ particles [27]. The size of the particles were in the range of 5-50 µm. Thus SEM study confirms the formation of ferric hydroxide particles. The images also demonstrate almost agglomerated shape.

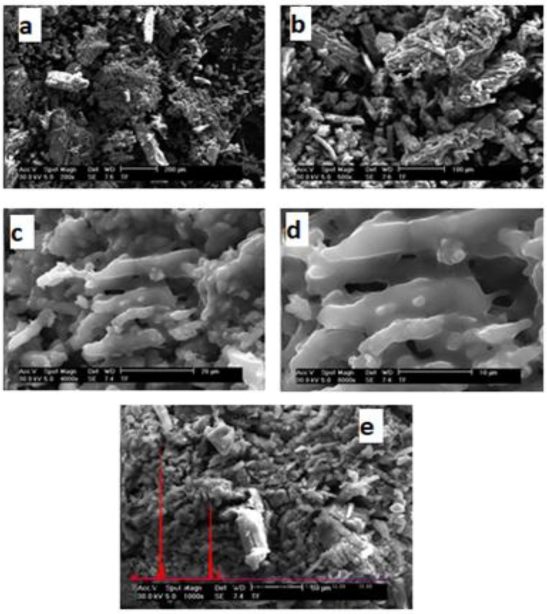

Figure 6. SEM images a.200X magnified, b. 500X magnified, c. 4000X magnified, d. 8000X magnified and EDX pattern of evaporated pregnant solution.

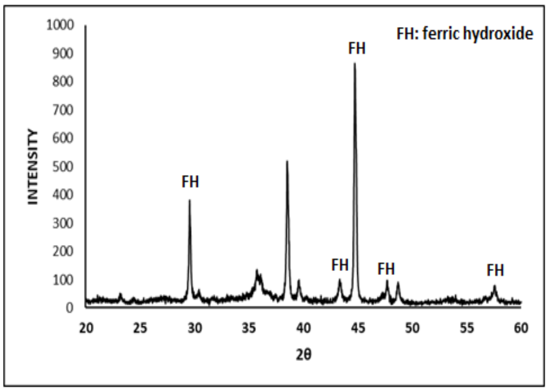

Figure 7. XRD pattern of alkaline precipitated pregnant solution.

4. Discussion

Chemical and physical characterization of oxide scale sample was done by XRD, SEM, EDX and volumetric titration analysis. Magnetite, wustite, metallic iron and silicon di-oxide are the main phases of the sample. The chemical composition of the sample consists of 70.88% Fe, 25.85% O and 3.27% Si. The morphologies of oxide scale sample were investigated by SEM analysis that are formed in lamellar, brittle, thin and plate forms. Considerable portion of particles grown as orthogonal or cornered (angular shaped).

As a result of leaching experiments for the production of iron (III) ions volumetric titration results showed that the amount of Fe^{+2} and Fe^{+3} could reach respectively %47 and %38 at 60°C temperature in 6N HCl acid concentration during 60 minutes leaching time. The XRD analyzes was done for the leach residue while the pregnant solution obtained under optimum leach conditions was saved for the next precipitation and evaporation processes. In the XRD pattern, it was seen that the metallic iron could not be dissolved and the silica remained in the leach residue as desired. It was determined that the source of iron ions in the pregnant solution came from magnetite and wustite in the oxide scale sample. In this context, the leaching optimization tests should be continued to ensure that the metallic iron can be dissolved but the silicon remains in the residue.

As a result of the evaporation process for the iron (III) chloride, $FeCl_3$ production was supported by Fe, Cl and O in the EDX results and with the $FeCl_3$ peaks in the XRD pattern (Figure 9). However, the reasons and types of other peaks seen in the XRD pattern should be studied to obtain pure $FeCl_3$.

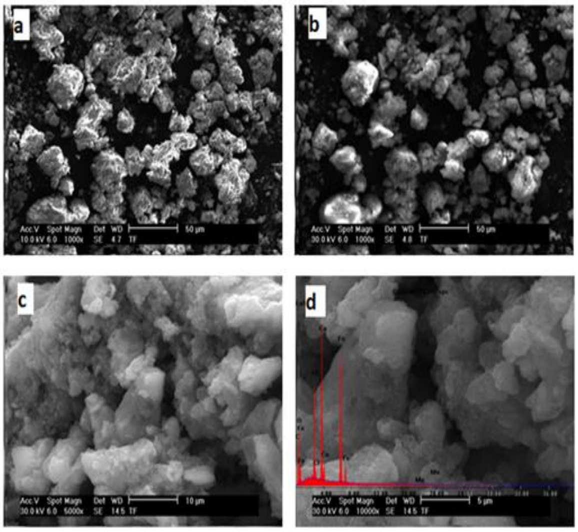

Figure 8. SEM images a.1000X magnified, b. 1000X magnified, c. 5000X magnified, d. 10000X magnified and EDX pattern of precipitated pregnant solution.

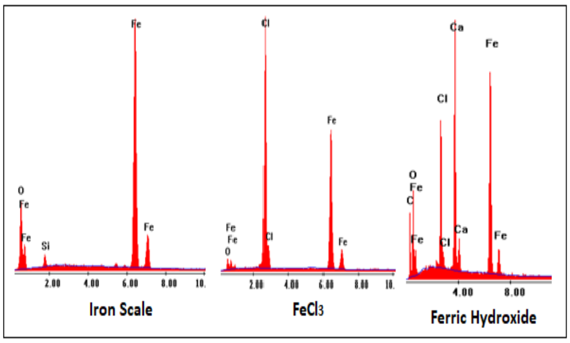

Figure 9. EDX analyzes of raw iron scale, $FeCl_3$ and Ferric hydroxide.

For the production of ferric hydroxide, the pH of the pregnant solution was increased to 11.5 to obtain the precipitate. In XRD pattern, ferric hydroxide and Ca complexes peaks were observed. Similarly, EDX analysis was also supported by the presence of Fe, O, Ca and C (Figure 9). The presence of Ca, C and Ca complexes in the XRD and EDX results is probably due to the use of industrial lime in the reaction process which was not removed completely or using excessive amount.

When looking at the SEM images, it was determined that the needle particles of $FeCl_3$ were caused by thermal treatment of evaporation. In the ferric hydroxide SEM images, it was based on the fact that the unformed granular structures formed during the deposition of the nano-sized core structures were agglomerated and collapsed as a large grain.

References

1. American Chemistry Council. "Chlorine Chemistry Division: Ferric Chloride: Clearing the stuff out of water." americanchemistry.com: Chemistry is essential2living - The American Chemistry Council N.p., Sept. **2003**. Web. 20 Sept. 2010. <http://www.americanchemistry.com/s_chlorine/science_sec.asp?CID=1258&DI D=4738&CTYPEID=113>.
2. Citulski, J., Khosrow F. and Fraser K. "Optimization of phosphorus removal in secondary effluent using immersed ultrafiltration membranes with in-line coagulant pretreatment — implications for advanced water treatment and reuse applications." Journal of Environmental Engineering and Science **2009**, 36, 1272-1283.
3. Stumm, W., and Morgan J.J. Chemical Aspects of Coagulation. Jour. AWWA, **1962**, 54(8) 71-994.
4. Stumm, W., and Melia, C.R.O. Stoichiometry of Coagulation. Jour. AWWA, **1968**, 60(5):514-539.
5. Black, A.P. Electrokinetic Characteristics of Hydrous Oxies of Aluminum and Iron. In Principles and Application of Water Chemistry. Edited by S.D. Faust and J.V. Hunter. New York: John Wiley and Sons. 1967.
6. Johnson, P.N., and Amirtharajah A. Ferric Chloride and Alum as Single and Dual Coagulants. Jour. AWWA, **1983**, 75(5):232-239.
7. Matijevic, E., and Janauer, G.E. Coagulation and Reversal of Charge of Lyophilic Colloids by Hydrolyzed Metal Ions. II. Ferric Nitrate. J. Colloid Interface Sci., **1966**, 21(2):197-223.
8. Phosphorous Removal from Wastewater. Water Treatment and Purification - Lenntech. Lenntech, **2009**,Web.1,March,2010.http://www.lenntech.com/phosphorous-removal.htm>.
9. Tang, H-X. and Stumm, W.,. The Coagulating Behaviors of Fe(III) Polymeric Species—I and II. Water Research, **1987**, 21(1):115-128.
10. California Water Technologies. “Phosphorus Removal." California Water Technologies. N.p., **2004**.Web.2,Oct.,2010. www.californiawatertechnologies.com/pdf/PhosphorousRemovalBulletin.pdf
11. Dejian, D., Hao, P., Wangjun, P., Yaowei Y., Guangxin, W., Jieyu, Z., Isothermal hydrogen reduction of oxide scale on hot-rolled steel strip in 30 pct H2-N2 atmosphere. International Journal of Hydrogen Energy, **2017**, 42, 29921-29928.
12. West, G.D., Birosca, S., Higginson, R.L., Phase determination and microstructure of oxide scales formed on steel at high temperature. Jour. Microsc. 2005, 217, 122–129. https://doi.org/10.1111/j.1365-2818.2005.01409.x
13. Chen, R.Y., Yuen, W.Y.D. Review of the High-Temperature Oxidation of Iron and Carbon Steels in Air or Oxygen. Oxidation of Metal, **2003**, 59, 433–468.
14. Weihua, S. Tieu, A.K., Zhengyi, J.,Cheng, L., Zhu, H., Surface characteristics of oxide scale in hot strip rolling. Journal of Materials Processing Technology, **2003**, 140 (1-3):76-83.
15. Higginson, R.L., Roebuck, B, Palmiere EJ., Texture development in oxide scales on steel substrates. Scripta Materialia, **2002**, 47:337–342.
16. Barrie, J and Hallbergs, K. B., Acid mine drainage remediation options: a review. Science of the Total Environment, **2005**, 338, 3-14.
17. Magnone E., Kim S. D., Park J.H., A systematic study of the iron hydroxide-based adsorbent for removal of hydrogen sulphide from biogas. Microporous and Mesoporous Materials **2018**, 270, 155–160.
19. Nisachon, N. K., Sirilak, Y., Thanasak, N., Adhesion behaviour of scales on hot-rolled steel strips produced from continuous casting slabs. Materials Today: Proceedings, **2018**, **5**,9359–9367 (The 10th Thailand International Metallurgy Conference (The 10th TIMETC)).
20. Guan C, Li J, Tan N, He YQ, Zhang SG., Reduction of oxide scale on hot-rolled steel by hydrogen at low temperature. Int J Hydrogen Energy, **2014**, 39:15116e24.
21. Shi J, Wand DR, He YD, Qi HB, Wei G., Reduction of oxide scale on hot-rolled strip steels by carbon monoxide. Mater Lett., **2008**, 62:3500e2.
22. Yang, Y.U., Chang W., Lin W., Jin C., Ya-jun H., Chang-ku S., Combination Effect of Si and P on Tertiary Scale Characteristic of Hot Rolled Strip Mater. Journal of Iron and Steel Research, International, **2015**, 22, 3,232-237.

23. Nilsonthi, T., Oxidation behaviour of hot-rolled Si-containing steel in water vapour between 600 and 900°C. Materials Today: Proceedings **2018**, 5,9552–9559 (The 10th Thailand International Metallurgy Conference (The 10th TIMETC)).
24. Ghosh, A. Chatterjee, A., Ironmaking and steelmaking: Theory and practice, Prentice Hall of India, **2008**, New Delhi, India.
25. Hiroaki, I., Shogo S., Nobuyuki I. and Hiroshi Y., Synthesis and characterization of intercalated few-layer graphenes. Japanese Journal of Applied Physics **2014**, 53, 02BD04.
27. LingFeng D., Yuan H., Xiang H., Xin C.S.W.D.G, Nifang Z., Yue L., Yanan S. and Wei S., Versatile method for the synthesis of porous nanostructured thin films of conducting polymers and their composites. Royal Society of Chemistry, **2015**, 5, 34616.
28. Gracien B.E., Joseph K.K.L., Omer M.M., Jérémie L.M., Jean-Felix S.Y., Peter K.M., Gamma irradiation inducing the synthesis of magnetic Fe3O4 nanorod particles in alkaline medium. International Journal of Materials Science and Applications, **2014**, 3(6), 339-343.
29. Hefa C., Weipu X., Junliang., Huanjun W., Yanqing H., Gang C., Pretreatment of wastewater from triazine manufacturing by coagulation, electrolysis, and internal microelectrolysis. Journal of Hazardous Materials **2007**, 146, 385–392.